Applied Acoustics 150 (2019) 5–13

Contents lists available at ScienceDirect

Applied Acoustics

journal homepage: www.elsevier.com/locate/apacoust

Inverted ultra-short baseline signal design for multi-AUV navigation

Dajun Sun [a,b], Jia Gu [a,b], Yunfeng Han [a,b,*], Jucheng Zhang [a,b]

[a] College of Underwater Acoustic Engineering, Harbin Engineering University, Harbin 150001, China
[b] Acoustic Science and Technology Laboratory, Harbin Engineering University, Harbin 150001, China

ARTICLE INFO

Article history:
Received 29 March 2018
Received in revised form 1 December 2018
Accepted 31 January 2019
Available online 13 February 2019

Keywords:
Multi-AUV
Collaborative positioning
iUSBL
Signal design

ABSTRACT

Recent years scholars have seen remarkable advancements in Autonomous Underwater Vehicle (AUV) technologies despite limited underwater energy. Multi-AUV positioning technology is an especially popular collaborative research subject; at present, long baseline and ultra-short baseline systems are available for multi-AUV positioning. Long baseline positioning has many disadvantages including overly complex settings and limited effective area for beacon collection.Ultra-short baseline positioning system is rather heavy and allows for fewer users.This paper proposes a new model based on the inverted ultra-short baseline (iUSBL) for AUV positioning. The model accommodates many users, maintains secret positions under deep sea conditions, and functions over lengthy distances, among other advantages. Highly detectable signals are designed for enhanced positioning accuracy in the proposed system. Simulation and anechoic tank experiment results indicate that the direct sequence spread spectrum (DSSS) signal is the optimal transmission signal during the positioning process.

1. Introduction

The AUV is a type of unmanned underwater vehicle (UUV) which is cable-free and highly agile, making it well-suited to underwater operations. It is an effective tool for ocean cognition and ocean exploitation and plays an important role in military reconnaissance, marine surveying and mapping, marine resource exploration, and other applications [24,17,9]. The single AUV is limited in capabilities and resources, while multi-AUV are highly flexible and efficient over a large detection range; they much more readily allow for long-term monitoring and rapid searching. The collaborative multi-AUV working mode has important research significance, to this effect [5,22]. In this working mode, precise multi-AUV collaborative navigation and accurate AUV locations are prerequisites for the proper functioning of the entire system [16].

The relative position between AUVs can be determined by various underwater acoustic positioning methods. Conventional methods of acoustic positioning include long baseline (LBL) and ultra-short baseline (USBL) methods [26,3,18,6]. The LBL positioning system consists of beacons placed on the seafloor and one transponder mounted on the carrier, which positions the carrier through the responses between them[13]. This method has a low positioning data update rate and is overly complex in terms of placement, calibration, and collection operations. Further, it only provides positioning services in fixed service areas and thus is not suitable for calculating the relative position between AUVs [25]. The USBL position system is composed of USBL arrays and transponders mounted on a carrier. It resolves positions according to the acoustic signal interaction between these components[14]. This method does not have the same shortcomings as LBL positioning, but still allows for only a limited number of users and causes heavy weight and high cost.

This paper presents a positioning system based on the iUSBL which achieves accurate positioning between multiple AUVs. A four-element array is mounted on the master AUV and each slave AUV only install a receive device in the positioning method. The system adopts a working mode by which a four-element array transmits signals and a target carrier receives four-channel signals [8].The multiple-input single-output positioning mode not only resolves the disadvantages of LBL but also has outstanding engineering advantages in three aspects. In terms of the system signal construction, it only needs to design four orthogonal signals to complete the positioning. In the aspect of real-time performance in engineering application, when the slave AUVs receive multi-channel signals sent from the main AUV, it can resolve or corrected the position directly, so that the real-time performance in positioning can be improved. In terms of the number of users that the system can carry, this system can carry a large amount of slave AUVs.

* Corresponding author at: College of Underwater Acoustic Engineering, Harbin Engineering University, Harbin 150001, China.
E-mail address: hanyunfeng_wd101@yeah.net (Y. Han).

https://doi.org/10.1016/j.apacoust.2019.01.033
0003-682X/

And each one only needs to receive signals from the master AUV, which avoid multiple signals collision problems occurring when many slave AUVs position at the same time.

The positioning method of the iUSBL system is similar to the USBL method [21]. Both involve obtaining the range and azimuth of the target by resolving the time delay. However, the time delay of the iUSBL system is obtained by analyzing four-way mixed signals of a single-track transmission. The superimposition of the four-way signal and the influence of environmental noise affect the accuracy of time delay estimations[12]. The proposed method includes a signal design which ensures accurate detection under the iUSBL system working mode to complete the transmission and improve the positioning accuracy between AUVs as much as possible.

Domestic and foreign scholars have deep research on multi-AUV collaborative positioning methods. Atwood proposed to apply LBL to multi-AUV collaborative navigation [1]. Vaganay improved this method and proposed the moving long baseline method (MLBL)[23], which greatly expanded the operational area of AUV. Larsen proposed the synthetic long baseline (SLBL) method by combining with INS [10,11]. Rigby studied the USBL method [19]. Cureio proposed the method of clock synchronization and one-way transmitting time (OWTT) distance measurement. At the same time, many estimation algorithms are introduced to improve the accuracy and precision of AUV navigation, such as extended kalman filter (EKF), particle filter (PF) and untracked kalman filter (UKF) [20].There have been relatively few truly fruitful produces on AUV positioning systems to date. The only sophisticated positioning product which exists currently is the AvTrak 6 positioning system developed by Sonardyne in the United Kingdom. [15]. AvTrak 6 combines transponder, transceiver, and telemetry link functions in one low-power unit which meets the requirements of a wide variety of AUV mission scenarios and vehicle types. The maximum depth of this system is 7 km, and its range accuracy is below 15 mm.

Multi-AUV collaborative navigation is a popular research subject across the globe. The goal of such research is accurately measuring the relative position of AUVs including their relative distance and azimuth. The present study was conducted to establish an iUSBL positioning model based on the master–slave multi-AUV working mode. A system platform was constructed to accomplish cooperation among AUVs. The positioning effects of the DSSS signal, frequency hopping (FH) signal, and COSTAS signal were assessed by comparison to determine the optimal transmission signal for highly accurate positioning within the proposed system framework.

2. System construction

An underwater positioning model based on iUSBL was designed in this study according to the requirements for collaborative multi-AUV navigation. The proposed method resolves the problem of relative position measurement between AUVs under the master–slave working mode of multi-AUV.

Collaborative multi-AUV navigation has a variety of working modes. The proposed system uses the master–slave mode to complete collaborative AUV navigation, as shown in Fig. 1 [4]. The master AUV is a pilot vehicle equipped with high precision navigation equipment including inertial navigation equipment, a Doppler velocimeter, GPS, depth transducer, and underwater acoustic communication equipment which provide high-precision positions in real-time. It has the ability to carry huge weight and energy.The slave AUV which follows the master AUV is equipped with low-cost navigation equipment and less energy. The master and slave AUVs share navigation information through the underwater acoustic communication device; the relative position between these AUVs can be used to complete the navigation process and precisely reveal the position of the slave AUV [2].

The relative position of the master-slave AUVs is solved by the iUSBL positioning system. The acoustic measurement device of the iUSBL system mainly consists of a four-element transmit array and a receiving hydrophone. The transmit array is mounted on the master AUV and one hydrophone is installed in each slave AUV. The range and azimuth between master and slave AUVs is calculated through the received four orthogonal coded signals of same frequency band from four arrays; the depth information is measured by depth transducer to obtain the relative position. A diagram of the positioning model is shown in Fig. 2.

Due to the small size of the array, it can be assumed that the receiving point is far away from the transmit device; that is, that the sound rays of each received signal are parallel. Under this assumption, the relative azimuth between AUVs can be obtained as follows.

$$\cos\theta_x = \frac{c \cdot \tau_x}{L} \tag{1}$$

$$\cos\theta_y = \frac{c \cdot \tau_y}{L} \tag{2}$$

where L represents the coaxial array distance, θ_x, θ_y are the target azimuths, and τ_x τ_y are the time delay difference of array elements on the x axis and y axis, respectively.

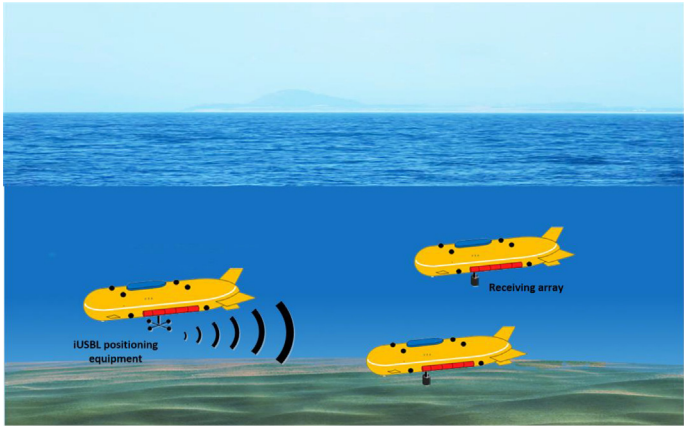

Fig. 1. Collaborative positioning diagram of master–slave AUVs.

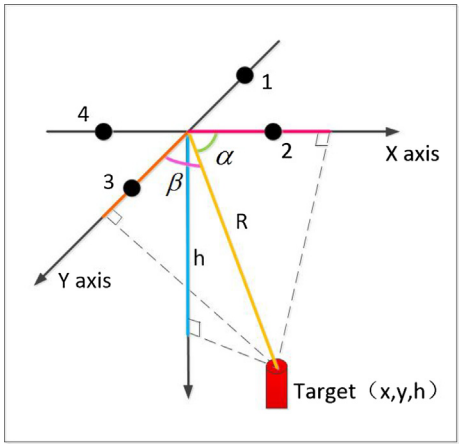

Fig. 2. Geometric Graph of Theoretical Position.

Based on the depth information of AUVs acquired by the depth transducer and the estimated azimuth information, the range and relative position between the master–slave AUV and can be calculated as follows.

$$R = \frac{z_s - z_m}{\sqrt{1 - (\cos\theta_x)^2 - (\cos\theta_y)^2}} \tag{3}$$

$$x = R \cdot \cos\theta_x \tag{4}$$

$$y = R \cdot \cos\theta_y \tag{5}$$

where R represents the target slant range, z_m, z_s are the depth information of the master and slave AUVs, and x, y are the position under the master AUV coordinate system.

The master AUV periodically broadcasts its own GPS coordinates. Each slave AUV is positioned through conversion of the coordinate system as per the master AUV's absolute position information and the relative position between AUVs. The slave AUV position information is calculated from the measured values z_m, z_s, τ_x, τ_y. Among these four measured values, the depth information z_m and z_s are obtained by the pressure sensor at especially high measurement accuracy. Therefore, the positioning accuracy depends on the accuracy of τ_x and τ_y. The master AUV sends four signals at the same time in the iUSBL system; this working mode causes multiple access interference (MAI) and multipath interference problems, which makes the delay estimation biased. It is necessary to design a signal that provides correct time delay estimations.

3. Signal design

The transmission signal plays a crucial role in the iUSBL positioning system. Signal performance directly affects the positioning performance in regards to anti-noise interference, multi-way interference, and anti-MAI. The ideal transmitted signal has sharp autocorrelation characteristics, zero cross-correlation, sufficient code sequences, and easy generation and implementation. According to these requirements, we compared the DSSS signal, FH signal, and COSTAS signal in this study. The FH signal completes the frequency shift keying modulation with the spread spectrum sequence. The DSSS is a common pseudo-noise code used to spread the spectrum of a signal at the transmitting terminal. The COSTAS sequence is a coding sequence in which the sub-pulses are mutually orthogonal. All three signals have strong autocorrelation and weak cross-correlation. We determined which is most suitable for the proposed AUV positioning system according to their respective autocorrelation and cross-correlation performance, time delay estimation performance, multipath interference resistance, and anti-MAI performance.

Signal parameter settings must be highly consistent to make the comparison among the signals meaningful. The parameters of the three signals mentioned above are shown below.

3.1. Autocorrelation and cross-correlation performance

Autocorrelation waveform characteristics are an embodiment of autocorrelation performance. Drawing the autocorrelation waveforms and its envelope of these three signals, including the sidelobe peak, reveals important differences in autocorrelation performance. Fig. 3 shows a comparison among the three signals we tested.

All three signals have the same peak value. The waveforms of the COSTAS and FH signal near the correlation peak are relatively similar and their first sidelobe values are larger than that of DSSS. The autocorrelation peak of the DSSS signal is sharp with a small (near zero) sidelobe value. Therefore, the DSSS signal performs best in regards to autocorrelation.

We also compared the autocorrelation peak-sidelobe ratio (PSLR) and cross-correlation interference ratio (CCIR) of each signal

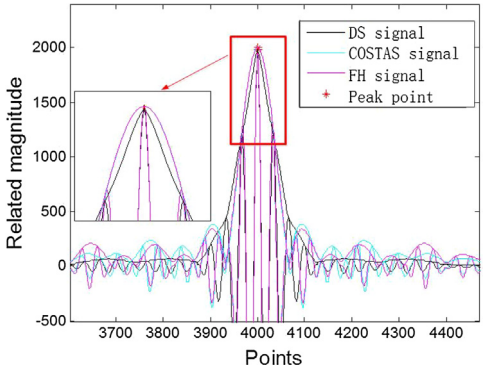

Fig. 3. Autocorrelation waveform comparison results.

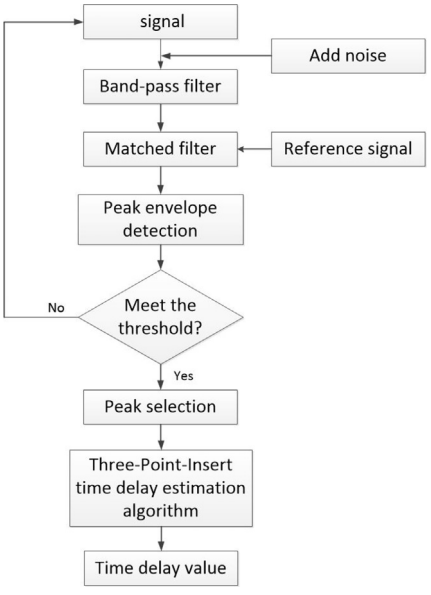

Fig. 4. Time delay estimation method flowchart.

to determine which is optimal in terms of signal superposition effects on the detection results. CCIR is defined as follows.

$$CCIR = \frac{P}{P_m} \tag{6}$$

where P is the signal autocorrelation peak value and P_m is the cross-correlation maximum value.

Larger PSLR represents better autocorrelation performance. The PSLR of the DSSS signal is much larger than those of COSTAS and FH signals, and the autocorrelation peak of DSSS signal is the sharpest. Therefore, the DSSS signal has optimal autocorrelation performance. A smaller CCIR also represents better autocorrelation performance–the FH signal has the largest CCIR and the DSSS signal has slightly less. By comparison, the DSSS signal has better autocorrelation and cross-correlation performance than the other two signals we tested.

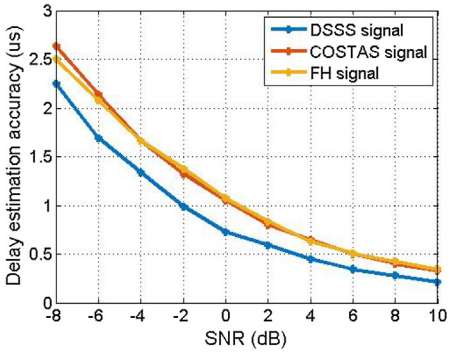

Fig. 5. Time delay estimation accuracy results.

3.2. Time delay estimation performance

We investigated anti-noise performance by comparing the time delay estimation among the three signals discussed above. The time delay estimation method we used is illustrated in Fig. 4.

The time delay estimation process is conducted in three steps. The first step is to roughly estimate the time delay by detecting the correlation peak of the signal with delay and reference signal information. Outliers are then removed via envelope detection and peak threshold restriction to ensure valid results. Finally, the three-point interpolation algorithm is used to correct the delay and obtain accurate estimations [7].

We added a constant delay and white noise to the simulation with different signal-to-noise ratios (SNRs) to the reference signal to create a received signal. We ran 1000 Monte Carlo simulations to obtain accurate time delays of the three signals with the estimation method detailed above.Fig. 5 shows the performance of these signals.

The accuracy of time delay estimation increases as SNR increases for any of the three signals. The COSTAS and FH signals yield virtually the same results – delay accuracy slightly lower than that of the DSSS signal under the same conditions. In theory, a sharper correlation peak represents higher time delay estimation accuracy. Our simulation results are in accordance with the theoretical results.

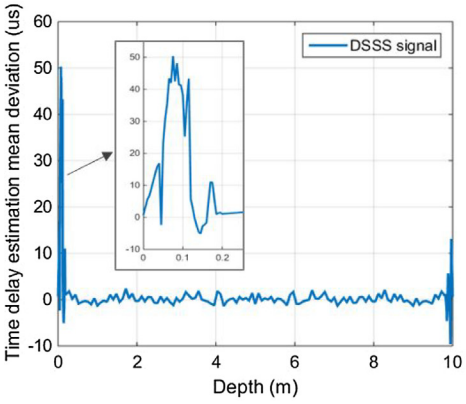

(a) Time delay estimation of DSSS signal

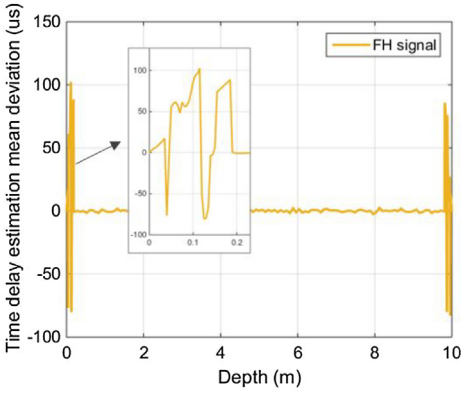

(b) Time delay estimation of FH signal

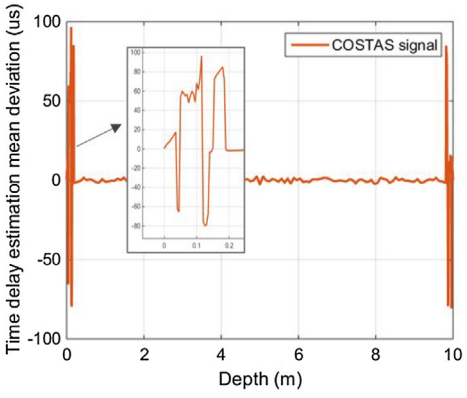

(c) Time delay estimation of COSTAS signal

Fig. 6. Maximum deviation of time delay estimation under multipath interference conditions.

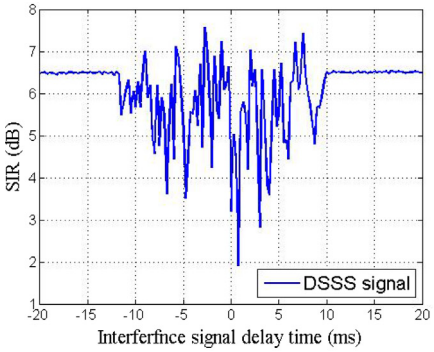

(a) MAI performance of DSSS signal

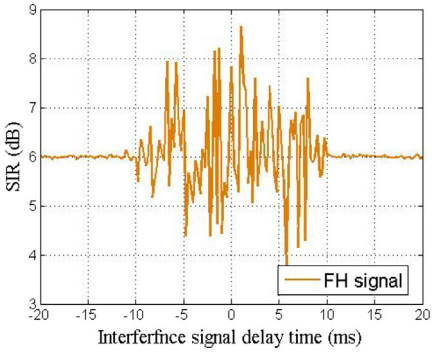

(b) MAI performance of FH signal

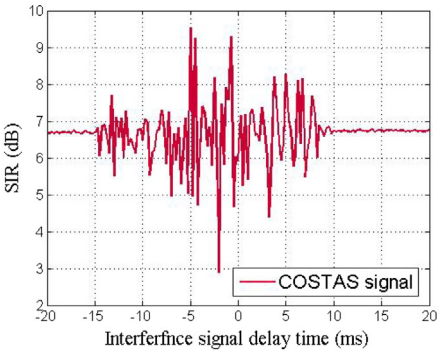

(c) MAI performance of COSTAS signal

Fig. 7. MAI performance of three signals.

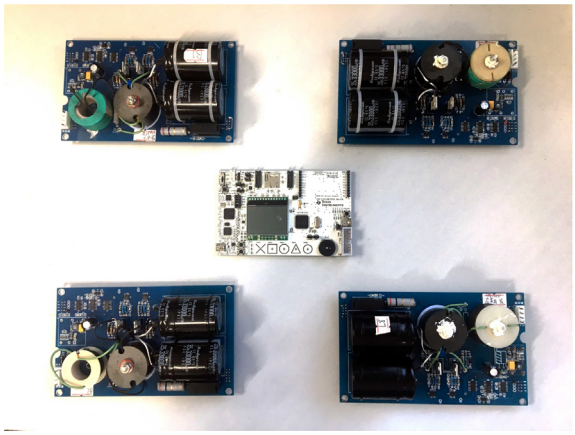

(a) iUSBL platform of controlling and launching

(b) iUSBL transducer array

Fig. 8. iUSBL system platform.

Table 1
Signal parameters.

Parameter	DSSS signal	FH signal	COSTAS signal
Pulse width (T)	10.017 ms	10 ms	10 ms
Bandwidth (B)	9–16(kHz)	9–16(kHz)	9–16(kHz)
Order (n)	6	8	8

Notes: DSSS sequence is restricted by its construction principle, so that its signal length is slightly different from the others.

Table 2
Autocorrelation and cross-correlation performance comparison.

Option	DSSS signal	FH signal	COSTAS signal
PSLR	14.71	7.71	7.13
CCIR	6.03	6.17	5.73

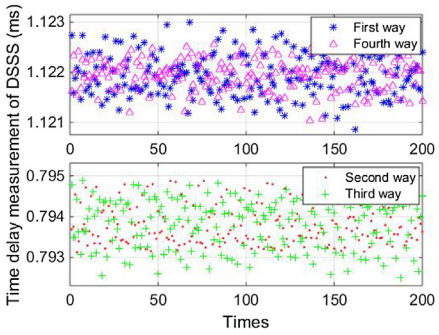

(a) Delay distribution of DSSS signal

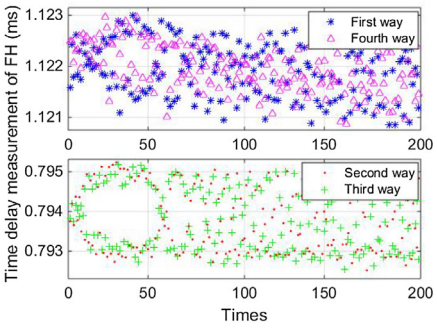

(b) Delay distribution of FH signal

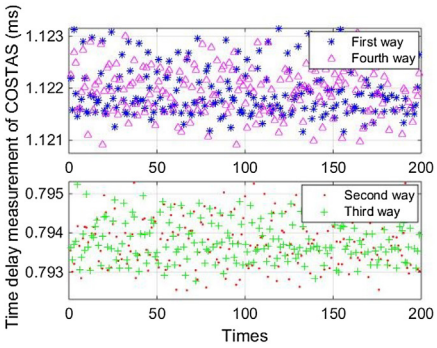

(c) Delay distribution of COSTAS signal

Fig. 9. The delay estimation result distribution of three signals.

3.3. Anti-multipath interference performance

The multipath effect makes the received signal repeatedly superimpose its own signal, which causes interference in the time delay estimation process. We investigated the anti-multipath interference ability of DSSS, FH, and COSTAS signals in terms of minimizing the multipath effects for accurate positioning.

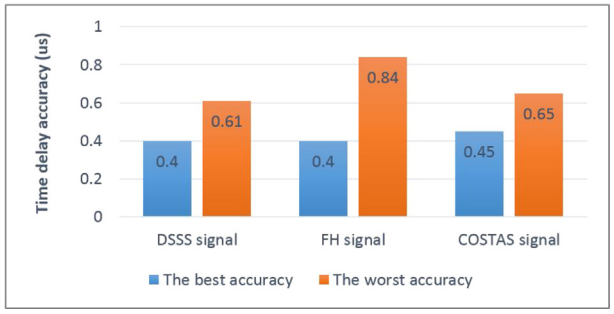

Fig. 10. The best and worst delay estimation results of the three signals.

To research multipath interference, we simulate the real acoustic channel environment in which the horizontal distance between transmitter and receiver is 5 m and the water depth is 10 m. Multipath interference is caused by the signal reflection of water surface and water bottom whose coefficients are set as 0.9 and 1. We then assessed the mean deviation of time delay estimation among the three signals using 1000 Monte Carlo simulations for each depth. The results are shown below.

Fig. 6 shows where the direct signal and multipath signal can be resolved after a 0.18 ms delay for all three signals by converting the depth to the delay difference between multipath signals and direct signal. The mean deviation of time delay estimation fluctuates as the multipath delay changes. By comparing the results, the performance of DSSS signal is superior to that of the other two signals.

3.4. Anti-MAI performance

MAI refers to multiple targets transmitting signals synchronously so that the signals are superposed. The detected signal is thus obscured and the accuracy of time delay estimation is degraded. We investigated the ability of DSSS, FH, and COSTAS

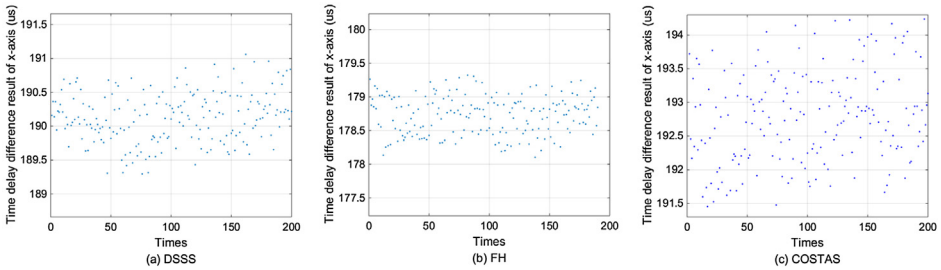

Fig. 11. The estimation result of the x-axis delay difference of three signals.

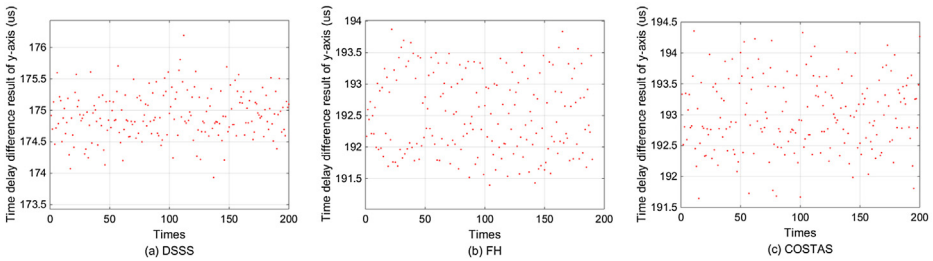

Fig. 12. The estimation result of the y-axis delay difference of three signals.

signals to resist MAI to select the best signal to complete the positioning process.

In the iUSBL positioning method, four arrays simultaneously transmit the same form of different address code signals at the same time; the received signal is composed of the detected signal and the other three signals with different delays. We assume the other three signals to have the same power as the detected signal and analyzed the signal to interference ratio (SIR) accordingly to compare signal performance. SIR is calculated as follows.

$$SIR = 10 * lg\left(\frac{C}{I}\right) \tag{7}$$

where C is the power of the signal correlation peak and I is the maximum sidelobe power caused by the interfering signal.

The results of 1000 Monte Carlo simulations are shown below.

According to the simulation results in Fig. 7, the SIR of all three signals vary as the interfering signal's time delay varies. SIR fluctuates more intensely when the delay is between −10 ms and 10 ms. Signal performance tends toward stability as the delay increases. The three signals show effectually the same anti-MAI performance, but in descending order as: COSTAS, DSSS, and FH with the mean SIR as the standard. These results are in accordance with the CCIR results discussed above.

Our results altogether suggest that the DSSS has favorable autocorrelation performance, good cross-correlation performance, and excellent anti-noise, anti-multipath interference, and anti-MAI capabilities. To this effect, the DSSS signal is optimal for iUSBL positioning.

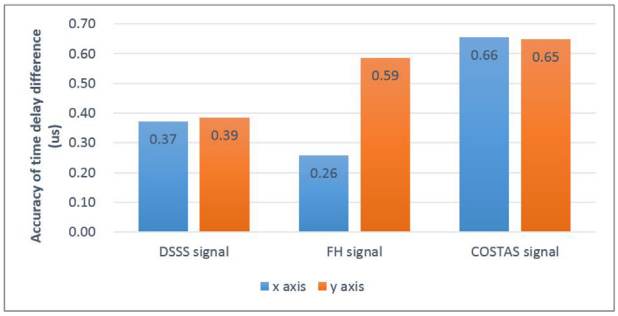

Fig. 13. The estimation accuracy of the coaxial delay difference of three signals.

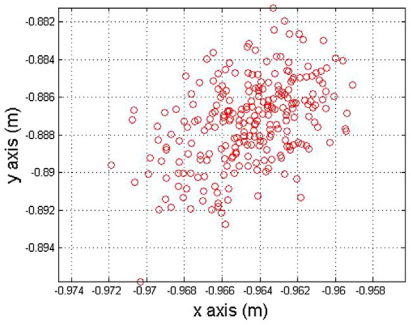

(a) Target position bitmap of DSSS signal

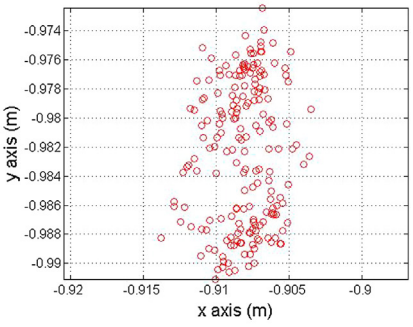

(b) Target position bitmap of FH signal

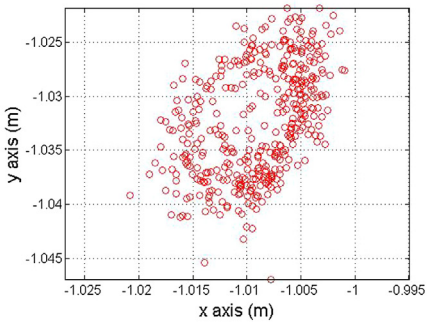

(c) Target position bitmap of COSTAS signal

Fig. 14. Target position bitmap of three signals.

4. Experimental verification

According to the simulation analysis results discussed above, we built a hardware platform of the iUSBL positioning system and tested the signal performance as-sampled in the tank environment to analyze the actual application of the proposed method.The iUSBL hardware system consists of an MSP430 integrated board, four launch boards, an iUSBL transducer array, a standard hydrophone, and a digital acquisition device. The MSP430 integrated board generates signals and controls the operation of the launch boards. The launch boards are connected to the transducer array to convert electrical signals to acoustic signals. The receiving device collects the received signal and uploads them to the PC. The standard hydrophone receives data collected by a digital acquisition device and upload it to the computer. The transducer array and hydrophone were respectively arranged 1.5 m and 3.5 m below the surface of the water for the sake of our experiment with a 1.5 m horizontal range located on the angular bisector of two array elements.The SNR of transmitting signal is set to 5 dB which depends on the poor condition that may occur in the lake or sea trials. The signal source level is adjusted by it, and the four element arrays transmits acoustic signal simultaneously to complete the positioning.Photographs of the experimental system are provided in Fig. 8.

In the tank trial, we used the hardware platform to transmit DSSS, FH, and COSTAS signals (Table 1) for 200 times with each sequence to compare the accuracy of time measurement, coaxial time delay difference, and positioning. We calculated the delay measurement results of DSSS, FH, and COSTAS signals, and compared their delay fluctuation. The figure below shows the delay measurement distribution results of these three signals (Table 2).

Fig. 10 shows the best and worst delay accuracy statistics for the three signals.

Depending on the relative position between the receiver and transmitter, the accuracy of the time delay measurement can be verified. Since the receiving array is located at an intermediate position between the two transmitting arrays, the first path delay and the fourth path delay value are approximated, and the second path delay value and the third path delay value are approximated. The distribution in Fig. 9 is caused by environment noise. In other words, the experimental and simulation results are consistent. As shown in Fig. 10, the DSSS signal has favorable accuracy among the three signals followed by the COSTAS and FH signals. The delay accuracy of COSTA and FH is essentially the same, but the COSTAS signal is much better than the FH signal in terms of data processing because COSTAS has good cross-correlation features and the ability to transmit four-way signals simultaneously.

The positioning result is calculated from the time delay difference in the coaxial array from formula 1. The coaxial time delay difference distribution result is shown as follows. Fig. 13 shows the coaxial time delay difference accuracy result of these three signal forms (Figs. 11 and 12).

Comparison among the experimental and calculated results also indicates that the accuracy of the time delay difference of each signal form is better than I2 times the worst-case simulation, which is

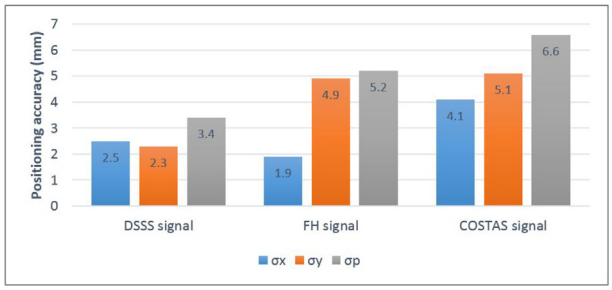

Fig. 15. Positioning accuracy result of the three signals.

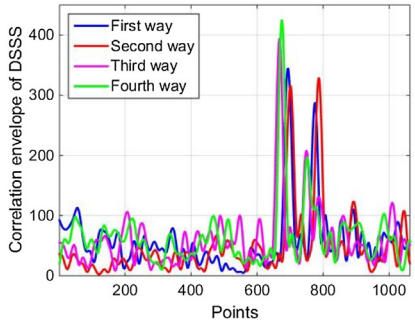

(a) The correlation envelope of DSSS signal

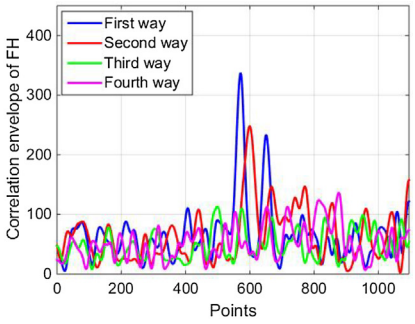

(b) The correlation envelope of FH signal

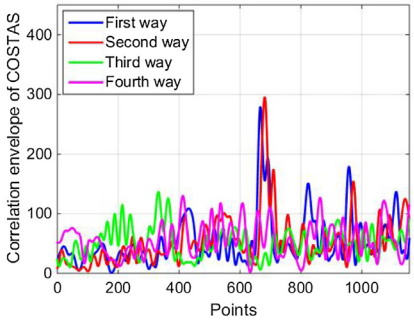

(c) The correlation envelope of COSTAS signal

Fig. 16. The correlation envelope among three signals.

in close agreement with the theoretical results as well. The time delay difference is subtracted from the time delay of the coaxial arrays, so elimination (or overlay) phenomena cause variations in the delay results. We determined that the DSSS signal yields the most accurate delay difference.

We next calculated the target positions by the collected four-way signals. Each target position was resolved several times to obtain a target position bitmap with signals collected continuously. The bitmaps are shown below (Fig. 14).

The statistical results for positioning accuracy are shown in Fig. 15.

According to the above experimental results, the positioning performance of DSSS signal is the best. And the position distribution is consistent with the x-axis and y-axis delay distributions, and again are in accordance with the relevant theories (Fig. 16).

In order to verify the detection performance of the DSSS, FH and COSTAS sequence, we use the hardware platform in Fig. 8 to test in the lake test environment. When the position of the target in the iUSBL emission array coordinate system is (4 m, 7 m, 6 m), the following figure shows the correlation detection result at this position.

The SNR of the lake test environment is about 5 dB, and the lake test environment is relatively complex. By comparing the signal detection results, it can be found that DSSS sequence can be detected 4-channel signals correctly with a large peak amplitude. Some signals in FH and COSTAS cannot be accurately identified, and their correlation peak amplitude is relatively small, which makes it difficult to detect. According to the above processing results, the detection performance of the direct spread sequence is the best.

By analyzing the time measurement accuracy, time delay difference accuracy, positioning accuracy and detection performance of three signals, we found that DSSS outperforms the others in regards to experimental, simulated, and theoretical analyses. The DSSS signal can be effectively applied as the iUSBL transmission signal.

5. Conclusion

Multi-AUV cooperative work is meaningful in regards to hydrological information collection, submarine mineral resource exploitation, underwater search and rescue operations, and many other applications. AUV positioning technology is the foundation of AUV cooperative work. This paper proposed a novel positioning model based on iUSBL that is applicable to a master–slave AUV positioning system. The slave mode is resolves self-positioning in real-time, accommodates a large number of users, functions across long distances, and has simple system structure, among other advantages. A DSSS signal capable of effective transmission, favorable correlation performance, and accurate delay estimation is designed and validated to provide the AUV system with highly accurate and useful positioning information.

Acknowledgments

This work was supported by the Key Program of the National Natural Science Foundation of China (Grant Nos. 61531012, 61801137, 61601134), State Key Laboratory of Ocean Engineering (Shanghai Jiao Tong University) (Grant No. 1701), National Natural Science Foundation of China (Grant No. 61701132), the Heilongjiang Science Fund for Distinguished Young Scholars of China (Grant No. JC2016013) and foundation (Grant No. 2017QD0047).

References

[1] Atwood D, Leonard J, Bellingham J, Moran B. An acoustic navigation system for multi-vehicle operations. International Symposium on Unmanned Untethered Submersible Technology. University of New Hampshire-Marine Systems; 1995. p. 202–8.
[2] Bahr A, Walter MR, Leonard JJ. Consistent cooperative localization. In: IEEE International Conference on Robotics and Automation. p. 4295–302.
[3] Caiti A, Corato FD, Fenucci D, Allotta B, Costanzi R, Monni N, Pugi L, Ridolfi A. Experimental results with a mixed usbl/lbl system for auv navigation. Underwater Communications and Networking. p. 1–4.
[4] Edwards DB, Bean TA, Odell DL, Anderson MJ. A leader-follower algorithm for multiple auv formations. Autonomous Underwater Vehicles, 2004 IEEE/OES. p. 40–6.
[5] Fiorelli E, Leonard NE, Bhatta P, Paley DA, Bachmayer R, Fratantoni DM. Multi-auv control and adaptive sampling in monterey bay. IEEE J. Oceanic Eng. 2004;31(4):935–48.
[6] Guerrero-Font E, Massot-Campos M, Negre PL, Bonin-Font F, Codina GO. An usbl-aided multisensor navigation system for field auvs. In: IEEE International Conference on Multisensor Fusion and Integration for Intelligent Systems. p. 430–5.
[7] Huang J. An interpolation algorithm of the correlation peak for time delay estimation. Appl. Acoust. 1996.
[8] Jakuba MV, Kinsey JC, Partan JW, Webster SE. Feasibility of low-power one-way travel-time inverted ultra-short baseline navigation. Oceans. p. 1–10.
[9] Kirkwood WJ. Auv technology and application basics. Oceans. pp. 15–15.
[10] Larsen MB. High performance doppler-inertial navigation-experimental results. Oceans, vol 2. p. 1449–56.
[11] Larsen MB. Synthetic long baseline navigation of underwater vehicles. Oceans, vol 3. p. 2043–50.
[12] Li Z, Dosso SE, Sun D. Joint inversion for transponder localization and sound-speed profile temporal variation in high-precision acoustic surveys. J. Acoust. Soc. Am. 2016;140(1):EL44.
[13] Li Z, Dosso SE, Sun D. Motion-compensated acoustic localization for underwater vehicles. IEEE J. Oceanic Eng. 2016;41(4):840–51.
[14] Li Z, Zheng C, Sun D. Track analysis and design for ultra short baseline installation error calibration. Oceans. p. 1–5.
[15] S. Ltd, Avtrak 6 positioning system.http://www.sonardyne.com, 2018.
[16] Maczka DK, Gadre AS, Stilwell DJ. Implementation of a cooperative navigation algorithm on a platoon of autonomous underwater vehicles. Oceans. p. 1–6.
[17] Paull L, Saeedi S, Seto M, Li H. Auv navigation and localization: a review. IEEE J. Oceanic Eng. 2014;39(1):131–49.
[18] Ribas D, Ridao P, Mallios A, Palomeras N. Delayed state information filter for usbl-aided auv navigation. In: IEEE International Conference on Robotics and Automation. p. 4898–903.
[19] Rigby P, Pizarro O, Williams SB. Towards geo-referenced auv navigation through fusion of usbl and dvl measurements. Oceans. p. 1–6.
[20] Rui G, Chitre M. Cooperative positioning using range-only measurements between two auvs. Oceans. p. 1–6.
[21] T. Tan, Underwater localization and navigation technology, in: National Defense Industry Press, 2007.
[22] Turner RM, Rode S, Gagne D. Distributed context-based organization and reorganization of multi-auv systems. Nucl. Acids Res. 2014;16(13):5863.
[23] Vaganay J, Leonard JJ, Curcio JA, Willcox JS. Experimental validation of the moving long base-line navigation concept. Autonomous Underwater Vehicles, 2004 IEEE/OES. p. 59–65.
[24] Wei-Feng MA, Zhen HU. Current researches and development trend on auv. Fire Control Command Control 2008.
[25] Zhang L, Demin XU, Liu M, Yan W. Cooperative navigation of multiple auvs using moving long baseline. Robot 2009;31(6). 581–585+593.
[26] Zhang T, Chen L, Li Y. Auv underwater positioning algorithm based on interactive assistance of sins and lbl. Sensors 2015;16(1):42.